On the Reliability Assessment of Artificial Neural Networks Running on AI-Oriented MPSoCs

Transient induced tungsten melting at the Joint European Torus (JET)

J.W.Coenen[a] G.F. Matthews[b], K.Krieger[e], D.Iglesias[b], P.Bunting[b], Y.Corre[e], S.Silburn[b], I. Balboa[b], B.Bazylev[g], N.Conway[b], I. Coffey[b], R.Dejarnac[d], E.Gauthier[e], J.Gaspar[i], S.Jachmich[b],,R.Scannell[b],M.Stamp[b], P.Petersson[j], R..A.Pitts[f], S.Wiesen[a],A.Widdowson[b], K.Heinola[h], A.Baron-Wiechec[b], and JET Contributors**

[a]*Forschungszentrum Jülich GmbH, Institut fr Energie- und Klimaforschung-Plasmaphysik, Partner of the Trilateral Euregio Cluster (TEC), D-52425 Jülich*

[b]*CCFE, Culham Science Centre, Abingdon, OX14 3DB, UK*

[c]*CEA, IRFM, F-13108 Saint-Paul-Lez-Durance*

[d]*Institute of Plasma Physics CAS, Za Slovankou 3, 18200 Praha 8*

[e]*Max-Planck-Institut f. Plasmaphysik, Boltzmannstr. 2, D-85748 Garching*

[f]*ITER Organization, Route de Vinon-sur-Verdon, CS 90 046, 13067 St. Paul Lez Durance*

[g]*Karlsruhe Institute of Technology, D-76021 Karlsruhe*

[h]*University of Helsinki, PO Box 64, FI-00560 Helsinki*

[i] *IUSTI UMR 7343 CNRS, Aix-Marseille University, 5 rue Enrico Fermi ? 13453 Marseille*

[j]*Fusion Plasma Physics, Royal Institute of Technology (KTH), SE-100 44 Stockholm, Sweden*

Abstract

Melting is one of the major risks associated with Tungsten. PFCs in tokamaks like JET or ITER are designed such that leading edges and hence excessive plasma heat loads deposited at near normal incidence are avoided. Due to the high stored energies in ITER discharges, shallow surface melting can occur under insufficiently mitigated disruption and ELM power load transients.

A dedicated program was carried out at JET to study the physics and consequences of W transient melting. Following initial exposures in 2013 (ILW-1) of a lamella with leading edge, new experiments have been performed on a sloped surface (15° slope) during the 2015/2016 (ILW-2) campaign. This new experiments allows significantly improved IR thermography measurements and thus resolved important issue of power loading in the context of the previous leading edge exposures. The new lamella was monitored by local diagnostics: spectroscopy, thermography and high resolution photography in between discharges. No impact on the main plasma was observed despite a strong increase of the local W source consistent with evaporation. In contrast to the earlier exposure, no droplet emission was observed from the sloped surface. Topological modifications resulting from the melting are clearly visible between discharges on the photographic images.Melt damage can be clearly linked to the IR measurements: the emissivity drops in zones where melting occurs.

In comparison with the previous leading edge experiment, no run-away melt motion is observed, consistent with the hypothesis that the escape of thermionic electrons emitted from the melt zone is largely suppressed in this geometry, where the magnetic field intersects the surface at lower angles than in the case of perpendicular impact on a leading edge. Utilising both exposures allows to further further test the model of the forces driving melt motion which successfully reproduced the findings from the original leading edge exposure.

Since the ILW-1 experiments, the exposed misaligned lamella has now been retrieved from the JET machine and post mortem analysis has been performed. No obvious mass loss is observed. Profilometry of the ILW-1 Lamella shows the structure of the melt damage which is in line with the MEMOS predictions allowing further model validation. NRA Analysis shows a ten fold reduction in surface deuterium concentration in the molten surface in comparison to the non molten part of the lamella.

1. Introduction

Tungsten W) is among the main candidate-plasma facing components (PFC) for a fusion reactor [1] and will be exclusively used in the ITER divertor[2]. Melting is one of the major risks associated with the material and so PFCs in tokamaks like JET or ITER are designed in such a way that leading edges and hence excessive plasma heat load ($q_{||}$) are avoided. It was shown during multiple experiments [3, 4] that deep W melting can cause severe damage to components and can degrade plasma performance [5]. In 2013 experiments [6, 7, 8] were performed to asses how transient melting during ELMs might affect the operation of JET and potentially ITER. The high stored energies of which ITER will be capable means that even with all PFC edges protected, shallow surface melting can still occur under disruption and ELM transients. The impact and physics of melting need to be studied in a relevant environment. JET is

able to produce transients / ELMs large enough (> 300 kJ per ELM) to facilitate melting of W. Such ELMs are comparable to mitigated ELMs expected in ITER [9].

In 2013 (ILW-1) a dedicated misaligned element (lamella) was installed in one part of the bulk W outer divertor, using a tapered exposed edge (0.25 – 2.5 mm) allowing exposure to the full parallel heat flux ($q_{\|}$). For the 2013 experiments the conclusion was that plasma impact was minimal and that melt layer motion was inline with the predicted melt layer modelling. It also opened up questions about the interpretation of IR measurements Discrepancies were apparent in the JET experiment between the parallel heat flux required to reproduce the misaligned lamella surface temperature and that derived from observations on non-misaligned surfaces. So called mitigation factors, or perhaps more correctly, reduction factors (0.2 for L-mode and 0.4 for H-mode [7, 8]) were derived from these measurements by using MEMOS-3D to generate temperature profiles based on the input heat fluxes and from them producing synthetic signals to compare with the IR data

In a joint international effort new experiments [10] have thus been aimed at both further elaborating the influence of transient melting on edges and surfaces, but also to elucidate the issue of power loading of edges [11] and IR interpretation. A crucial point with respect to all experiments is the temperature evolution of the exposed lamella and its front surface and hence the actual relation of heat fluxes to the melt behaviour and melt layer motion. One particular experiment in ASDEX Upgrade [12] was designed as companion experiment to the JET exposures to also measure the thermo-electric emission [13, 14, 15] causing melt layer motion in fusion devices [3, 4, 16, 17, 18, 19].

In this contribution the general overview of the experiments for the ILW-2 exposure (2015/2016) will be given together with the rational linking the old and the new exposure. Material damage evolution, material losses and plasma impact are discussed. Issues related to the actual $q_{\|}$) determination are presented and compared to the ILW-1 experiment. The presentation of the new experiments is followed by an update on the postmortem analysis of the old ILW-1 2013 edge lamella. Here the main focus lies on the surface characterisation and metallography.

2. Setup

Due to power handling considerations [20] the outer divertor is split up in four so-called Stacks (A,B,C,D) with A being located closest to the High Field Side (HFS). Figure 1 displays a view onto divertor modules with its four stacks. Each Stack is split in a number of individually shaped lamellas [20]. The lamellas have a poloidal extent of 5.9cm and are 5.5mm wide toroidally. Stack A is used for exposing the specialised Lamellas for these experiments as operation at JETis usually contained to the Low Field Side of the horizontal target namely Stack C & D.

When considering both experiments two special lamellas were used. a Leading Edge and sloped Lamella (Fig. 2).

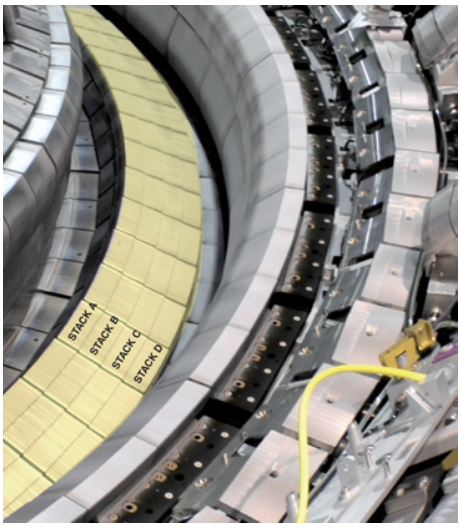

Figure 1: Modules of the JET outer divertor depicting the position of the dedicated lamella.

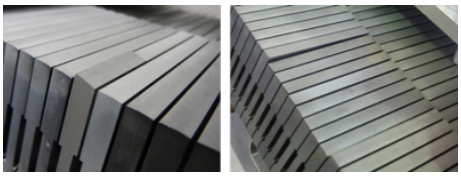

Figure 2: Dedicated lamellas for both experiments - as instaled

The toroidal installation position of the lamellas during both experiments was chosen to allow the existing IR diagnostics [21, 22] to be used. For the first experiment (ILW-1) the special lamella was designed to allow significant preheating due to the front surface being exposed to the parallel heat flux [7]. The exposure to the parallel heat flux is achieved by producing a chamfered leading edge of 0.25-2.5mm and also lowering of the 8 lamellas in front of the exposed edge to mitigate potential shadowing (fig. 1). This top viewing of the IR diagnostic did however mean that during the ILW-1 exposure only the propagation of the heat pulse into the lamella from the side could be observed [7, 8].

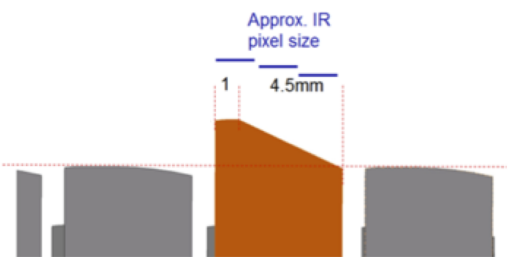

Figure 3: New IR View

For the second experiment the issue about IR interpretation was taken into account. It was determined that it was necessary to use a geometry where simple power factors are more likely to

apply and also a direct observation of melt zone by IR was possible. This was aimed at an easy access to the parallel heat-flux $q_{||}$. In figure 3 the rational for the lamella shape is given. With the resolution of the IR being in the oder of one mm the aim was to allow for multiple data points along a sloped surfaces. The sloped surface (15° slope) in the bulk W outer divertor is contained to the high-field side part (2cm) of the Stack A lamella used.

In order to quantitatively interpret the outcome of the experiment and also be able to follow the progress of potential melt damage several other diagnostics were employed. To be able to monitor changes to the installed lamella a high-resolution camera was installed (SBIG ST-8300 Monochrome [23]). With a resolution of ~ 100 μm one can clearly follow the evolution of the lamella and the surrounding areas.

A direct observation of the emitted W from either evaporation or droplet emission is realized by a localised viewing cord as installed during both experiments [7]. A small observation volume covering the area of the special lamella and part of Stack A allows dedicated measurements. Based on the WI 400.88nm line one can calculate the released amount of W as demonstrated in [24, 3]. In the interest of brevity we would refer to previously published work for the previous experiments in 2013 for the details [7, 8].

3. ILW-2 Experiments

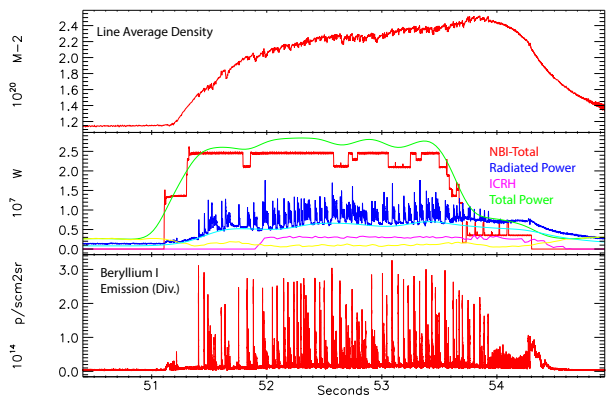

Figure 4: Pulse Overview for the ILW-2 Melt pulse #91965

A sequence of 3.25MA/2.7T H-Mode JET pulses with 27MW input power and regular Type-I ELMs (P_{ped} ~ 12kPa) was used to obtain repeated, transient melting (melt depth 5-10 μm) of a the modified sloped W lamella.

As shown in fig. 4 both Neutral Beam and ICRH were employed to reach the total heating power. In fig. 4 also traces for the line average density and the Beryllium I emission from the divertor are given. The density is reasonably stable during the exposure of the Stack A lamella between 51.5 and 53.5s. The ELM characteristic, given by the BeI signal is not as even between the individual ELMs as desired but did allow a successful experiment.

In figure 5 the details for the strike-line position are given. The exposure duration of the lamella was increased to increase the base temperature and allow transient melting by the heat-flux originating from the individual ELMs in line with the ILW-1 exposures [7]. By increasing the exposure duration the base temperature was increase following a simple sqrt(t) relation as expected.

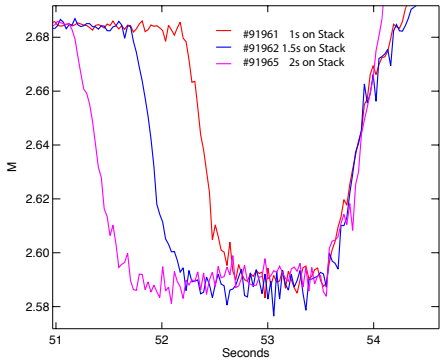

Figure 5: Exposure of sloped lamella given by strikeline position

During #91965 the base temperature together with the ELM heatflux was enough to facilitate melting. Figure 6 shows one example of the HF calculated for the individual ELMS and the phase in-between ELMS.

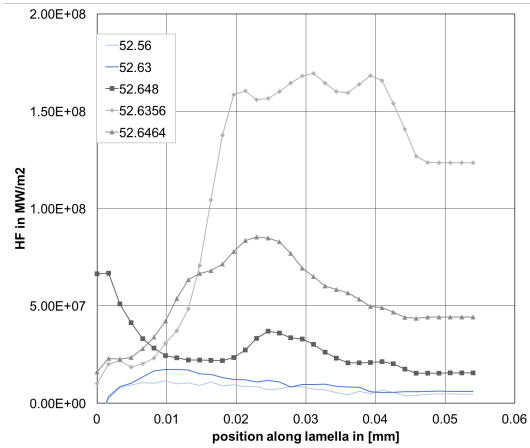

Figure 6: Heat-Flux calculated for #91965. The maximum heat-flux corresponds to the peak ELM heat-flux whereas the blue curves show the inter-ELM period.

When looking at the heat-flux deposited during this particular ELM it becomes clear that the extend of the slope introduced is marginal in terms of exposure area. Only the ELM heat-load between 0 and 0.2 cm is impacting the sloped part of the special lamella.

This fact can be clearly seen also in figure 7. On the left the Infrared emission from the sloped part is clearly visible above the non sloped part. On the right hand side the lamella is shown, undamaged and damaged. When looking carefully also the fact actual melting can be determined from the IR pictures. in the bottom IR image lower emissivity from the molten mirror like surface cause the IR emission to drop and thus make the damage visible in the IR.

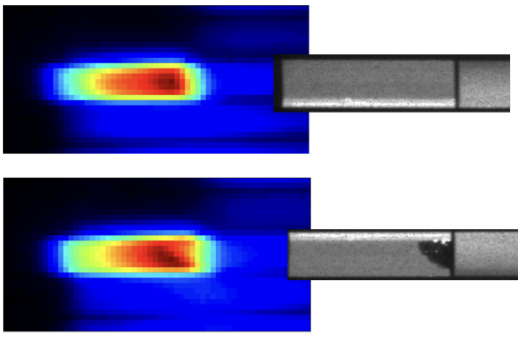

Figure 7: Lamella and Lamella Damage is given in comparison to the IR-emission footprint.

Topological modifications resulting from the melting are clearly visible between discharges on the photographic images. No run-away melt motion is observed. To elaborate a bit more clearly the damage inflicted figure 8 is used. Differential pictures are produced always subtracting subsequent images.

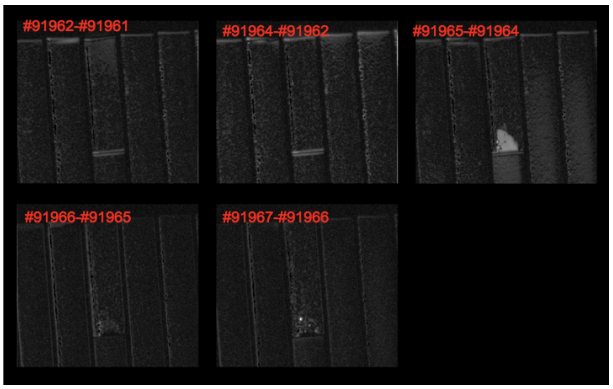

Figure 8:

Clearly the appearance of the melt damage during #91965 can be observed. Subsequent Pulse, with lower energy input did only produce minor surface modification. Thus only one melt pulse was achieved. The behaviour is quite different from the layer droplet produced in the ILW-1 exposures [7]. From previous experiments and modelling it is assumed that the dominant forces leading to this material redistribution are related to a thermo-electric current driven jxB force, as seen from previous melt experiments [13]. From recent collaborative experiments in ASDEX Upgrade it is however assumed that the escape of thermionic electrons emitted from the melt zone seems largely suppressed in a more sloped of flat geometry [12, 10]. The much lower net current then leads to a reduced jxB force on the melt, poloidal melt motion is considerably reduced. Instead, other forces, probably dominated by surface tension as the melt layer repeatedly re-solidifies, produce the observed final corrugated surface topology.

In addition to the surface damage it is also of crucial interest to study the impact of the melt damage onto the plasma operation. During the 2013 ILW-1 exposure droplet emission was observed, likely due to the large acceleration of the melt.

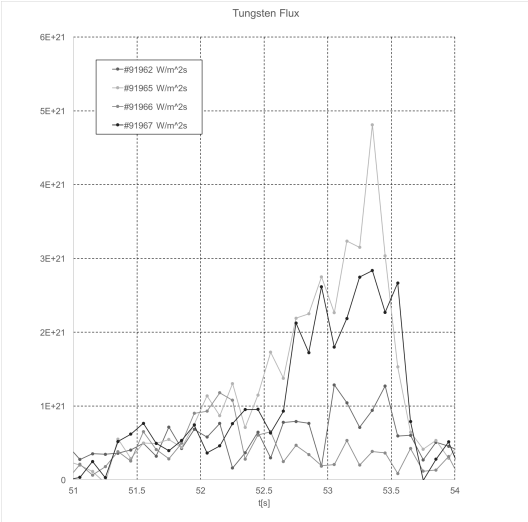

Figure 9: W emisson based spectroscopic measurements on top of the exposed Lamella.

For the new sloped lamella no droplets impacting the plasma were found. Only a rise in W emission (fig. 9) consistent with evaporation was found (~1E22 1/(m^{2}s)) [25]. The emission measured is typical for evaporation fluxes at the given melt temperature of 3695 K. the influx rises as the temperature increase.

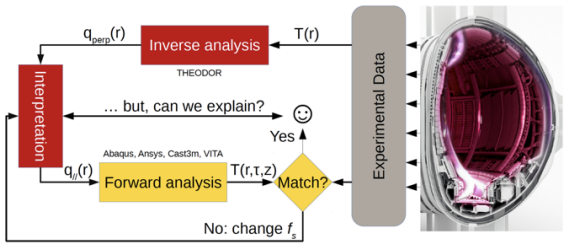

Figure 10: Scheme of forward and inverse analysis to match modelling approaches and finalise the determination of the parallel heatflux.

One of the main aims of the experiment was to tackle the so called mitigation factors required to match experiment and modelling [7, 8]. L-Mode required a mitigation factor of 0.2, while H-mode required a mitigation factor of 0.4 on the parallel heat-flux to match experimental data on temperature rise.

Fig. 10 shows the actual issues face and tackled. Typically an inverse analysis is performed to determine the perpendicular heat-flux on the impinged surface. Using this heat-flux one should then be able to calculate the temperature evolution using forward analysis based on finite element methods. A very detailed analysis of geometrical factors was undertaken [26] and also detailed forward modelling was performed [26, 27]. It was show that, at least in L-mode, the assumption of optical heat flux projection is justified and for H-Mode the measured heat-flux can be reasonably well matched to allow forward modelling of the melt geometry. Using the same model and same plasma parameters, good agreement is obtained for all three geometries, validating the assumption of optical heat load projection after accounting for observed background on

the IR heat flux, the origin of which is still under investigation. This now provides a solid basis for modelling also the more complex ELMing H-mode conditions [27].

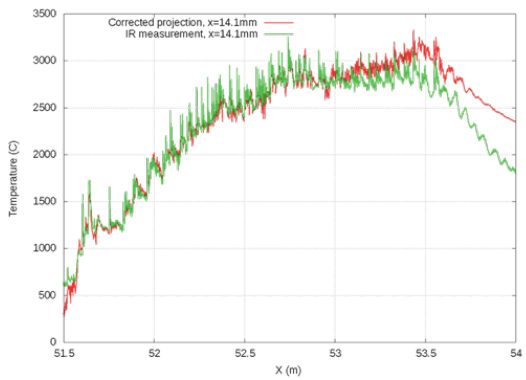

(a) Temperature Evolution: experimental(green) - forward modelling red

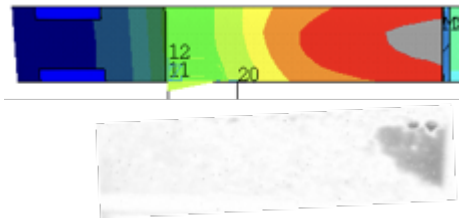

(b) Temperature footprint based on forward calculated temperatures vs melt damage

Figure 11:

Figure 11 shows a good match between the experimentally determined temperatures and the calculated ones based on the determined parallel heat-flux 11 (a) together with a geometric match between the temperature footprint and the actually damaged area. Further work is ongoiing , however it is clear that for both L-Mode and H-Mode accurate determination of geometries and incorporation of them into the models allows to explain the mitigation factors within the uncertainties. More details are given in [26, 27]

4. Post -Mortem Analysis - ILW-1 Leading Edge Lamella

Based on the long turn around time of components in JET only recently acces was possible to the leading edge lamella exposed in 2013. The main interest here is on the actual structure of the melt droplet and the melt redistribution as well as potential changes to the material structure. In addition information was gathered regarding fuel content of the re-solidified material.

In figure 12 the close up imagery of the lamella is given and can be compared to the documented melt evolution given in fig. 18 [7]. Already after the experiment a layer by layer growth of the damage was postulated utilising high resolution imagery, this can now be confirmed by fig 12. the melt material is transport from the central part of the lamella to the high-field side following the jxB force direction. A layer wise structure can

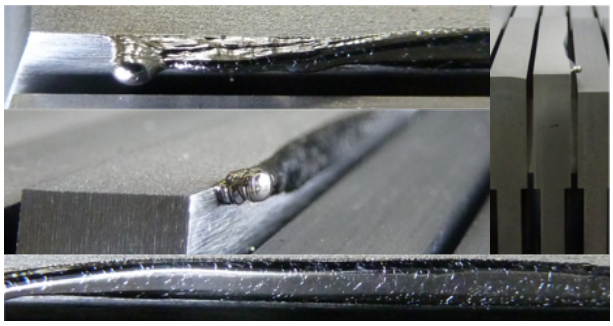

Figure 12: Close Up Photography of the resolidified melt layer for the ILW-1 leading edge exposure

be seen which is consistent with the amount of around 60-100 ELMs having caused the melting. Strong re-crystallisation of the material is evident already from the shiny top surface, large grains can be observed. The main droplet is actually attached to the leading side of the lamella as expected from a pure inward driven motion.

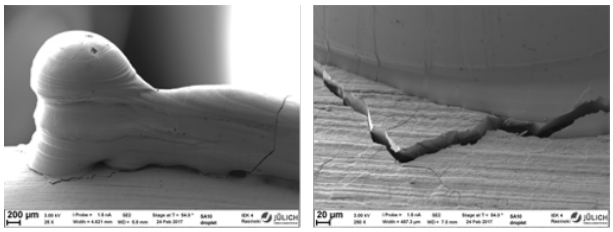

Figure 13: SEM Image of the droplet produced

Figure 13 gives a electron microscopy close up of the actual droplet. the intriguing detail here is the crack surrounding the droplet. Strong re-crystrallization and thus embrittlement is expected from re-solidified material. This means that a droplet when exposed to further heat-loads and thermal stresses might dislodge and enter the plasma. Depending on size and trajectory this can cause a plasma disruption. As seen in many of the deep melt experiments [5, 17, 28, 18, 3, 4] droplet emission can occur. This effect is usually attributed to melt layer motion ripping of droplets from the surface [13, 29, 30] as well as connected wave instabilities [31, 32] or boiling effects [28]. Typically the release of droplets clearly causes cooling of the core plasma and thus influences performance.

An attempt at determining the melt layer loss yielded at most 100mg of mass loss connected with an uncertainty of around 100% as the determination relies an volume based reference weight estimate. In addition the area is typically a net deposition are in JET. A deposition layer is formed on the lamella and the re-solidified melt of about 100nm in height mainly consisting of Be, C as well as traces of nitrogen. With respect to the retained fuel measurements were performed using 3He NRA at 2.8 MeV. It was found that the resolidified surface layer contains 10 times less (2E15 at/cm^2) of deuterium then the exposed unmolten area.

In a further step the profilometric measurements were performed to be able to match the melt layer redistribution mod-

elling with the actual material moved, in 14 the data is presented. Clearly the issue of reflection has limited the ability to

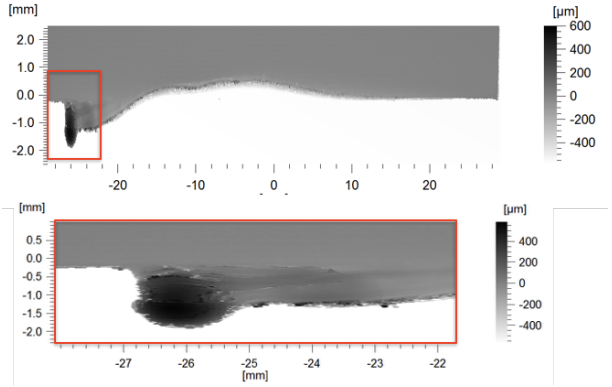

Figure 14: Pofilometer Data for the melt damage.

measure the depth near the melt layer damage and thus more an outline of the melt damage is visible. The material moved is in line with the previous estimation of around $6mm^3$ as determined in [7]. The droplet stand out 1.7 mm from the leading edge and contains nearly all of the material moved from the central part of the lamella.

This profile can now be compared with the Melt Layer Modelling by the MEMOS Code [13]. In fig. 15 6 consecutive melt pulses using the input data from 2013 were modelled in contrast to one pulse in the previous publication [7]. With the qualitative

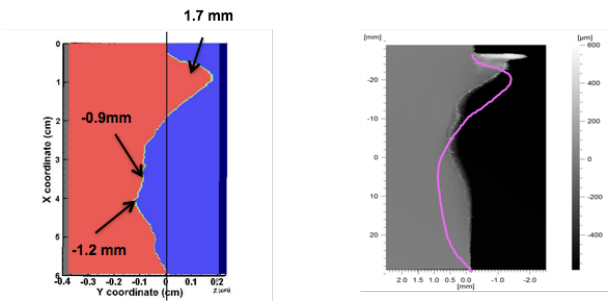

Figure 15: Updated Melt Layer Modelling after 6 consecutive pulses relevant for the 2013 exposure. (r) comparison to the actual profile measurement.

agreement documented before [7] the profilometry data now allows a quantitative comparison of the full melt experiment with the actual data. Here a deviation can be clearly observed. Work is ongoing to re-evaluate the heat-flux data used but also to improve the understanding of the model. Here especially also the experiment regarding the jxB forces and thermionic emission at ASDEX-Upgrade are crucial [12]

5. Summary

In conclusion it can be said that the experiment successfully achieved transient melting in the desired geometry. The JET ELMs were of a size relevant to mitigated ELMs in ITER and shallow melting of sloped surfaces causes almost no visible plasma impact. The ILW-2 2015/16 experiment improved significantly the ability of IR analysis. No mitigation factor is required to understand the outcome of the experiments in L-Mode and the mitigation factors have mainly been identified as systematic uncertainties in the calculation. The ILW-2 2015/16 experiment did show that when exposing a sloped surface instead of a leading edge far less melt motion is ?visible - here the reduced effect of the jxB forces can be seen as main driver.

From the SEM possible during the post-mortem analysis of the ILW-1 2013 Lamella it can be seen that the droplet produced might eventually come of and potentially disrupt the plasma if exposed to future heat-flux It is observed that the surface structures seen on the droplets are partly reflected in the grain structure. A weight loss is not apparent from the postmortem measurement but can be expected as droplets were released during the 2013 experiments. Melting impacts the hydrogen retention - D is driven out of the 2013 lamella when compared to the non molten surfaces. From the EDX map of the flat lamella it is observed that Stack A as expected shows deposition of Be,C and other light elements. During the post mortem analysis of the ILW-12013 lamella a comparison with profilometry and MEMOS showed only small discrepancies

Obviously ITER has the potential to produce similar damage over the whole area of the strike point. The number of droplets produced could therefore be much larger especially for leading edges Whether or not this would be sufficient to disrupt an ITER plasma cannot be simply concluded but the JET results do provide the basis for such a calculation. The JET results are directly relevant to what would happen in the case of molten surface. The JET results also suggest that provided such an event is detected in ITER and is not repeated too many times such that large droplets build up, there would be no risk of a disruption

Acknowledgements

This work has been carried out within the framework of the EUROfusion Consortium and has received funding from the Euratom research and training programme 2014-2018 under grant agreement No 633053. The views and opinions expressed herein do not necessarily reflect those of the European Commission

[1] Coenen, J. et al. *Physica Scripta*, **2016** (2016), T167, 014002.
[2] Pitts, R. et al. *Journal of Nuclear Materials*, **438** (2013), S48.
[3] Coenen, J. W. et al. *Nuclear Fusion*, **51** (2011), 8, 083008.
[4] Krieger, K. et al. *Physica Scripta*, **T145** (2011), T145, 014067.
[5] Lipschultz, B. et al. *Nuclear Fusion*, **52** (2012), 12, 123002.
[6] Matthews, G. F. et al. *Physica Scripta*, **T167** (2016), T167, 014070.
[7] Coenen, J. et al. *Nuclear fusion*, **55** (2015), 2, 023010.
[8] Arnoux, G. et al. *Journal of Nuclear Materials*, **463** (2015), 415–419.
[9] Pitts, R. et al. *Journal of Nuclear Materials*, **415** (2011), 1 SUPPL, S957S964.
[10] Pitts, R. et al. *Nuclear Materials and Energy*, (2017).
[11] Gunn, J. et al. *Nuclear Fusion*, **57** (2017), 4, 046025.
[12] Krieger, K. et al. (2017). PFMC-2016 Conference Neuss.
[13] Bazylev et al., B. *Physica Scripta*, **T145** (2011), 014054.
[14] Sergienko, G. et al. *Physica Scripta*, **T128** (2007), 81–86.
[15] Garkusha, I. et al. *Journal of Nuclear Materials*, **363-365** (2007), 1021–1025.
[16] Coenen, J. et al. *Journal of Nuclear Materials*, **438** (2013), S27.

[17] Coenen, J. W. et al. *Fusion Science And Technology*, **61** (2012), 2, 129–135.
[18] Coenen, J. W. et al. *Journal of Nuclear Materials*, **415** (2011), 1, 78–82.
[19] Coenen, J. W. et al. *Physica Scripta*, **T145** (2011), T145, 014066.
[20] Mertens, P. et al. *Journal of Nuclear Materials*, **415** (2011), 943–947.
[21] Arnoux, G. et al. *Review of Scientific Instruments*, **83** (2012), 10, 10D727.
[22] Balboa, I. et al. *Review of Scientific Instruments*, **83** (2012), 10, 10D530.
[23] STF-8300M - https://www.sbig.com/products/cameras/stf-series/stf/stf-8300m/.
[24] van Rooij, G. et al. *Journal of Nuclear Materials*, **438** (2013), S42.
[25] T.Tanabe. *Atomic and Plasma-Material Interaction Data for Fusion*, **5** (1994), 129.
[26] Iglesias, D. *Nuclear Fusion*, **to be submitted** (2017).
[27] Corre, Y. et al. *Nuclear Fusion*, **57** (2017), 6, 066009.
[28] Coenen, J. W. et al. *Nuclear Fusion*, **51** (2011), 11, 113020.
[29] Bazylev, B. et al. *Fusion Engineering and Design*, **84** (2009), 2-6, 441–445.
[30] Bazylev, B. et al. *Physica Scripta*, **2009** (2009), T138, 014061.
[31] Miloshevsky, G. and Hassanein, A. *Nuclear Fusion*, **50** (2010), 11, 115005.
[32] Shi, Y.; Miloshevsky, G. and Hassanein, A. *Journal of Nuclear Materials*, **412** (2011), 123–128.